Journal Pre-proof

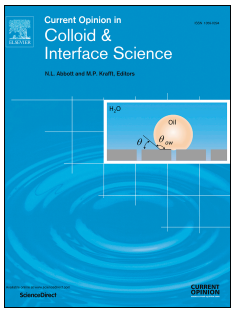

Contact angle hysteresis

Hans-Jürgen Butt, Jie Liu, Kaloian Koynov, Benedikt Straub, Chirag Hinduja, Ilia Roismann, Rüdiger Berger, Xiaomei Li, Doris Vollmer, Werner Steffen, Michael Kappl

PII: S1359-0294(22)00013-9

DOI: https://doi.org/10.1016/j.cocis.2022.101574

Reference: COCIS 101574

To appear in: *Current Opinion in Colloid & Interface Science*

Received Date: 14 September 2021

Revised Date: 10 January 2022

Accepted Date: 16 January 2022

Please cite this article as: Butt H-J, Liu J, Koynov K, Straub B, Hinduja C, Roismann I, Berger R, Li X, Vollmer D, Steffen W, Kappl M, Contact angle hysteresis, *Current Opinion in Colloid & Interface Science*, https://doi.org/10.1016/j.cocis.2022.101574.

Contact angle hysteresis

Hans-Jürgen Butt,[1,2] Jie Liu,[1] Kaloian Koynov,[1] Benedikt Straub,[1] Chirag Hinduja,[1] Ilia Roismann,[3] Rüdiger Berger,[1] Xiaomei Li,[1] Doris Vollmer,[1] Werner Steffen,[1] Michael Kappl[1]

[1] Max Planck Institute for Polymer Research, Ackermannweg 10, 55128 Mainz, Germany

[2] Tokyo Institute of Technology, Earth Life Science Institute, Chemical Evolution Laboratory Unit, Tokyo, Japan

[3] Institute for Fluid Mechanics and Aerodynamics, Technische Universität Darmstadt, Alarich-Weiss-Straße 10, 64287 Darmstadt, Germany

This manuscript is dedicated to honour our dear colleague and friend Peter Kralchevsky.

1. Abstract

In thermodynamic equilibrium the contact angle is related by Young's equation to the interfacial energies. Unfortunately, it is practically impossible to measure the equilibrium contact angle. When for example placing a drop on a surface its contact angle can assume any value between the advancing Θ_a and receding Θ_r contact angles, depending on how the drop is placed. Θ_a - Θ_r is called contact angle hysteresis. Contact angle hysteresis is essential for our daily life because it provides friction to drops. Many applications, such as coating, painting, flotation, would not be possible without contact angle hysteresis. Contact angle hysteresis is caused by the nanoscopic structure of the surfaces. Here, we review our current understanding of contact angle hysteresis with a focus on water as the liquid. We describe appropriate methods to measure it, discuss causes of contact angle hysteresis, and describe the preparation of surfaces with low contact angle hysteresis.

2. Introduction

Wolfgang Pauli (1900-1958) is credited of saying "*God made the bulk; surfaces were invented by the devil*." This saying does not leave much room for worse. If there is something worse, we will nominate "*contact angle phenomena"* first in line. In wetting we deal with three interfaces and three media that all meet at one line. While scientist have developed techniques to characterize interfaces, our repertoire of methods allowing to characterize the narrow region around the three phase contact line are fairly limited. Thus, the structure and dynamics on the nanometer and molecular scale at the contact line is largely unexplored. The fundamental problem is that the number of molecules at the contact line is intrinsically very small.

Still, contact angle phenomena influence our daily lives, occur in many natural phenomena and are relevant for numerous applications. Applications include printing, painting, coating, distribution of herbicides and insecticides, fogging of glasses and mirrors, condensation and evaporation in e.g. heat transfer systems, wetting of textiles and filters, flotation, oil recovery, powder dispersion, soldering and lubrication. Therefore, it is essential to quantitatively describe contact angle phenomena and make them predictable.

The starting point to quantify contact angle phenomena is to place a liquid drop on a solid substrate. For some surfaces the liquid spreads over the surface and forms a film. However, for other surfaces the drop spreads until a certain diameter is reached. At the contact line of the liquid, the solid and the air the liquid exhibits a certain slope. This slope is termed the contact angle (Figure 1).

More than 200 years ago Thomas Young considered the situation [1]. In the famous Young equation the equilibrium contact angle Θ_e is related to the interfacial free energy of the liquid-vapor γ_L, the solid-gas γ_S, and the solid-liquid interfaces, γ_{SL}:

$$\gamma_L \cos\Theta_e = \gamma_S - \gamma_{SL} \tag{1}$$

Macroscopically it can be derived by minimizing the free energy of a liquid in contact with a flat, inert, homogeneous and smooth solid surface [2-7]. Alternatively, one can consider the horizontal components of the interfacial forces acting on a virtual contact line; in equilibrium these forces should balance [6, 8-10]. Young's equation has been verified by Monte Carlo [11] and molecular dynamics simulations [12-14]. Experimentally, Young's equation cannot be verified because the solid surface energies γ_S and γ_{SL} cannot be measured independently (only changes in the solid surface energies can be measured) [3].

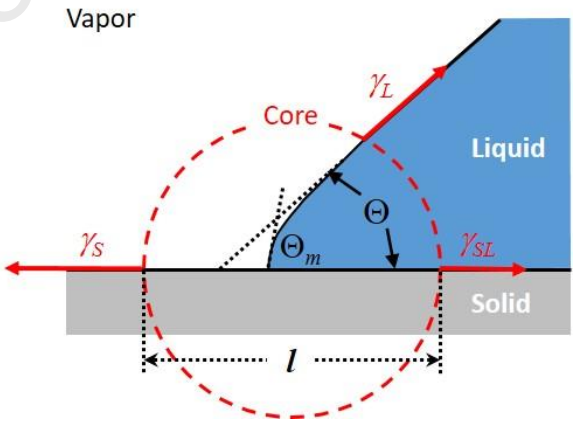

***Figure 1**. Schematic of the region around the contact line.*

One of the advantages of Young's equation is, that its derivation is independent on the atomistic structure of the liquid and solid surfaces at the contact line. In the vicinity of the contact line, in the so-called core region (Fig. 1), van der Waals or electric double layer forces may deform the free liquid surface [15, 16] or the solid may elastically deform [6, 17]. As long

as the structure in the core region is preserved upon a translation of the contact line, the macroscopically observed contact angle outside the core region can still be related to the far-field interfacial energies by Young's equation [3, 4]. Considering the range of surface forces the typical size of the core region is of the order of 0.1-1 µm. Consequently, the macroscopic contact angle is measured outside the core region and is accessibly by optical microscopy. In that sense, Young's equation does not care what actually happens near the contact line.

If not mentioned otherwise we refer to the macroscopic contact angle. Macroscopic contact angles are defined as a boundary condition for the liquid surface which in equilibrium is otherwise described by the Laplace equation. The contact angle is the angle the liquid surface forms with the solid surface when the interface is extrapolated to the contact line and by using the appropriate differential equation [18, 19].

When discussing heterogeneous, rough or structured surface it is useful to also define "apparent" contact angles [7, 20-22]. We define an *apparent* contact angle at a length scale much bigger than the surface structure or variations in its chemical composition. Corrugations in the liquid surface decay exponentially with a characteristic length given by the extension of the corrugation [19]. As for the macroscopic contact angle, the apparent contact angle is determined from the extrapolated contour of the liquid surface at the point of intersection with the substrate. Extrapolation in this case is carried out at a length scale larger than the surface structure.

As one example, the fluorine-doped tin oxide (FTO) surface shown in Figure 2A looks smooth bye eye or a normal camera. Images taken with a scanning electron microscope (SEM) reveal, however, a distinct structure on the 0.1-1 µm length scale (Fig. 2B). Therefore, the apparent contact angle would be defined for a length scale much larger than 1 µm. Some surfaces are even structured on different length scales. One example is the Lotus leaf. By eye, it looks relatively flat and planar (Fig. 2C). In the SEM one can distinguish two surface structures: Protrusions of ≈10 µm height and 20 µm spacing, which are covered with cylindrical nanofilaments of ≈100 nm diameter and 1 µm length (Fig. 2D-F).

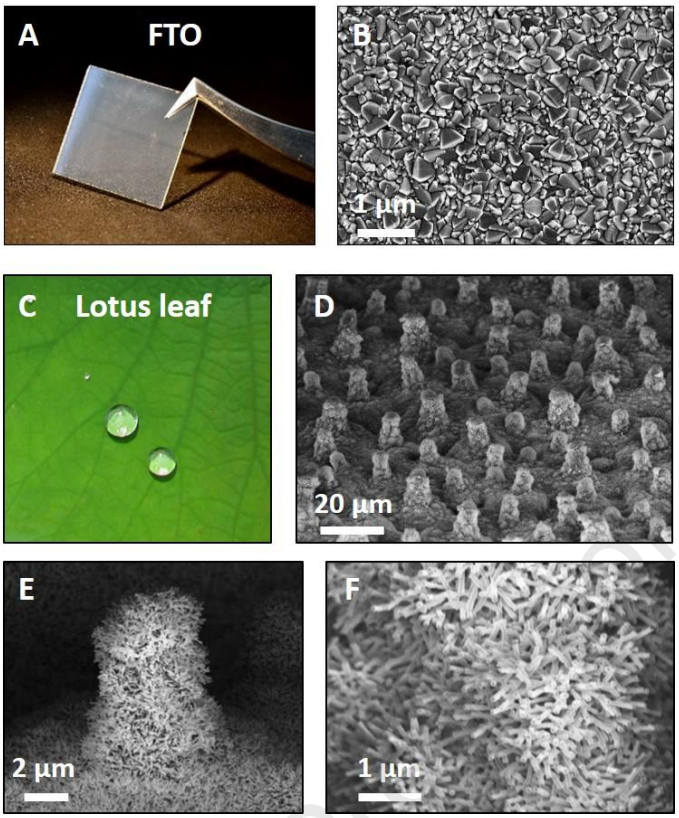

Figure 2. A fluorine-doped SnO2 (FTO) conductive glass (Sigma-Aldrich, 7 Ω/cm2) imaged with a normal camera (A) and a SEM (B). Surface of a Lotus leaf imaged with a normal camera (C) and with an SEM at different resolutions (D-F).

3. Advancing and receding contact angles

Early experiments showed that contact angles not only depend on the interfacial energies but also on the surface structure, the pretreatment of the surfaces and on contamination [23]. Agnes Pockels was to our knowledge the first to grasp the concept of an advancing and receding contact angle [24]. She noticed that the contact angle of an advancing liquid which had just stopped advancing is larger than the contact angle of a drop which was forced to recede. She also noticed that drops, where the difference between the two values is low, slide easily while drops with a large difference in advancing and receding contact angles do not slide at all when the substrate is being tilted. When measuring the surface tension of water by the capillary rise method, Harkins & Brown noted that “the rise for a falling meniscus was always greater than for a rising meniscus” [25]. In the 1920ies and 1930ies the concept of a receding and advancing contact angle which limit a range of actually reported contact angles for a specific liquid-substrate combination was established [26-29]. Contact angle hysteresis is observed on all solids, even on presumably flat, homogeneous and inert surfaces. The situation is a bit unsatisfactory because the ideal case described by Young’s equation can practically not be realized.

The measureable quantities which characterize a specific surface are the advancing and receding contact angles by Θ_a and Θ_r, respectively. The difference between the two is called contact angle hysteresis, $\Delta\Theta = \Theta_a - \Theta_r$. In general, both contact angles depend on the propagation speed of the respective contact line U. For this reason one needs to distinguish static and dynamic contact angles. To define the static values one can for example consider a sessile drop placed on a surface. The actual contact angle takes a value between the static advancing and receding contact angles, depending on how it is deposited. When we increase the actual contact angle, e.g. by increasing the volume of a drop, at some point the liquid front will start advancing. We define the characteristic angle just before the contact line advances as the static advancing contact angle ${\Theta_a}^0$. When decreasing the actual contact angle, e.g. by reducing the volume of a drop, at some point the liquid front will start to recede. We call the characteristic angle just before the contact line recedes the static receding contact angle ${\Theta_r}^0$. For water, static contact angle hysteresis $\Theta_a^0 - \Theta_r^0$ is typically larger 10°, even on seemingly smooth, homogeneous and rigid surfaces such as silicon wafers or freshly cleaved mica.

Alternatively one may define the advancing and receding contact angles from measuring the velocity dependence of contact angles at an advancing and receding liquid front and extrapolate to zero velocity [30], $\Theta_a(U \to 0)$ and $\Theta_r(U \to 0)$. It is not yet clear, that both definitions lead to the same values [31]. To distinguish the two, sometimes the adjective "static" or "recently" is added in the first case and "dynamic" is used in the second case.

Contact angle hysteresis exists because contact lines usually do not slide freely. Real solid surfaces are not perfectly homogeneous, flat, rigid and inert. Real surface are rough, amorphous, deformable, show different crystalline orientations or have defects. And they tend to be "contaminated". In air, real surfaces have water or hydrocarbons adsorbed. In that sense, any liquid wetting such a surface needs to replace the adsorbed layer. Furthermore, the precise structure of many materials depends on how they have been treated in the past. Silicon oxide (and glass) is a prominent example. Depending on its history, e.g. exposure to heat, water, chemicals, etc. it is more or less hydroxylated [32]. Surfaces may adapt to the presence of the liquid and change their structure. These factors lead to many metastable states of the contact line [33-37]. In a real wetting situation the contact line is in one of these metastable states and one cannot be sure, that it is in global thermodynamic equilibrium (Fig. 3). As a result, contact lines are pinned. To overcome contact line pinning, a certain force per unit line has to be applied. It is given by $\gamma_L(\cos\Theta_r - \cos\Theta_e)$ and $\gamma_L(\cos\Theta_e - \cos\Theta_a)$ for a receding and an advancing contact line, respectively.

To overcome metastability and reach global equilibrium, sessile drops have been mechanically vibrated. Irvine Langmuir already wrote that before reading the contact angle "the water drop was then placed on the surface and this was shaken and sometimes tilted slightly, so that the drop reached a stable shape" [38]. Later, researchers applied vibrations systematically [39, 40]. Typically the substrate was vibrated at amplitudes of 1-2 mm in normal direction. The idea is to use vibrations so that the contact line overcomes local energy barriers and settles at

equilibrium. Indeed, in a certain range of vibration excitations a "mean" contact angle $\overline{\Theta} = (\Theta_a + \Theta_r)/2$ is obtained. Sometimes also the mean contact angle is determined via the cosines: $\cos\widehat{\Theta} = (\cos\Theta_r + \cos\Theta_a)/2$ [40]. We believe that although one can avoid being trapped *far* away from equilibrium, even vibrations will not bring the whole contact line to its global equilibrium. When due to a certain vibration the contact line has found its global energy minimum position, the next vibration might kick it out of this position again (Fig. 3). For this reason Ruiz-Cabello et al. talk about the most stable contact angles reached by vibrations [41].

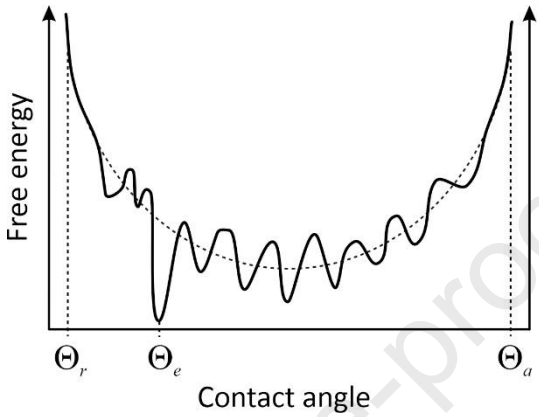

***Figure 3**. Schematic energy landscape diagram for the contact angle with multiple local minima.*

Contact angle hysteresis is not only a nuisance preventing us from measuring Θ_e. It has a direct and important consequence for everyday life: It provides friction to sessile drops. The lateral adhesion force required to slide a drop over a surface is [42-44]

$$F_c = w\gamma_L k(\cos\Theta_r - \cos\Theta_a) \qquad (2)$$

Here, w is the width of the contact area of the drop and $k \approx 1$ is a geometrical factor, which depends on the shape of the drop [44-49]. The value of k depends on details how the drop is deposited and k may even vary when the shape of the drop changes.

From Eq. (2) we see that without contact angle hysteresis, drops would slide down a tilted plane even at low tilt angles. A negligible lateral adhesion of drops may be nice for keeping glasses or windscreens of cars clean, prevent fogging, and allow an efficient removal of drops after condensation in heat exchangers. It would, however, be a nightmare for applications such as printing, painting, coating, distribution of herbicides and insecticides. Thus, contact angle hysteresis is of fundamental importance in our daily lives.

4. Measurement of contact angle hysteresis

Contact angle hysteresis can be measured with any technique available to measure advancing and receding contact angles. Examples are the capillary rise [25, 50, 51], the Wilhelmy plate [34, 52-58], vertical fibre or moving tape methods [59-61] (Fig. 4A). Most commonly, a sessile

drop is imaged by a video camera while the drop is inflated or deflated via, e.g., a micropipette (Fig. 4B) [62-68]. The same can be done with a captive bubble, in which case 100% humidity in the air phase is ensured [64]. With the sessile drop method even some information about dynamic contact angles can be obtained. It is limited to low velocity because otherwise the inflation/deflation may lead to disturbing flow inside the drop. In addition, one should keep in mind that the time, the surface has been in contact with liquid depends on the whole process. Thus, if the surface adapts, the dynamic receding contact angle may change because the surface had been in contact with liquid for some time [67, 68].

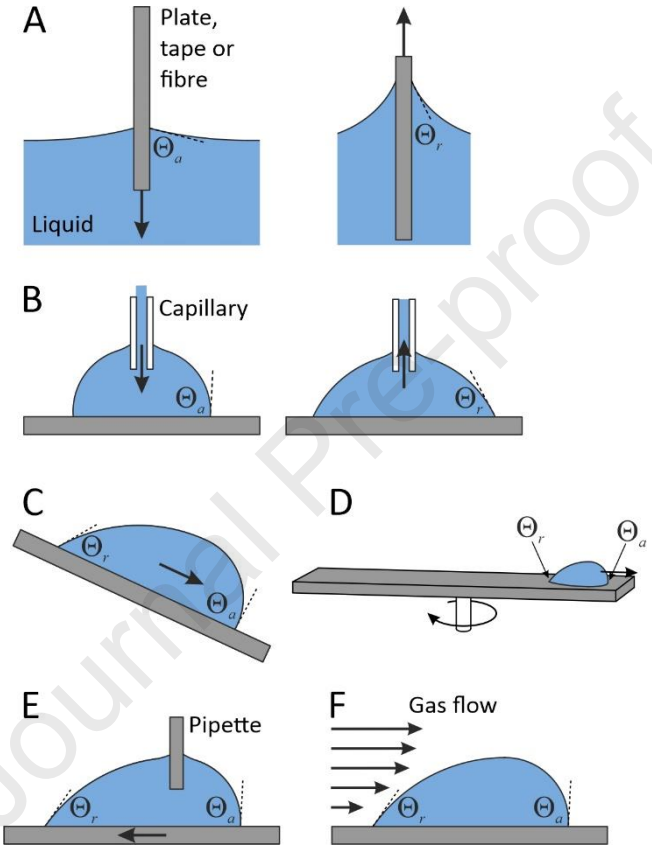

***Figure 4**: Schematic of experiments applied to measure advancing and receding contact angles. (A) Moving a plate or tape into a liquid or pulling it out of the liquid, (B) inflating and deflating a sessile drop, (C) tilted plate, (D) centrifuge, (E) drop adhesion forces instrument, (F) aerodynamic drag.*

A common method to measure advancing and receding contact angles is on a tilted plate (Fig. 4C) [42, 44, 69-73]. By inclining the supporting surface, gravity can gradually be increased until at some tilt angle the drops starts sliding. While tilting, the shape of the drop is observed by a camera. Afterwards, the contact angles are determined from the images taken just before the drop starts sliding. When setting this lateral adhesion force equal to the lateral component of the gravitational force, $mg \sin \alpha$, an expression for the sliding angle α of a drop is obtained [42, 44, 46, 69, 70, 74]:

$$\sin \alpha = \frac{w\gamma_L k}{mg}(\cos \Theta_r - \cos \Theta_a) \qquad (3)$$

Here, g = 9.81 m/s^2 is the gravitational acceleration, m is the mass of the drop. It is related to the drop volume V via the density ρ, $m = V\rho$. Since the width of the contact area usually scales with the radius of the drop, the right hand side of Eq. (3) scales with $V^{-2/3}$. Thus, the sliding angle α, also called roll-off angle, depends on the volume of a drop.

One disadvantage of the tilted plate method is that once the drop has started to move it is usually out of control. For this reason, only the static advancing and receding contact angles can be measured. To obtain dynamic contact angles the drop needs to be imaged during sliding, which again is technically more demanding than imaging a stationary sessile drops [73, 75, 76]. Usually such studies are carried out with liquids of high viscosity to decrease the velocity and make imaging easier.

If gravity is not sufficiently strong to cause sliding, the effect of mass can be enhanced by placing the drop on one arm of a centrifuge (Fig. 4D) [46, 77-79]. In this case the centrifugal force acting on the drop can be gradually increased by increasing the rotation speed. In the centrifuge smaller drops can be used than on a tilted plate. It is, however, technically more demanding to image the drop on a centrifuge.

In order to overcome technical limitations for observing sliding drops, the drop can be pinned to a fixture while the sample moves horizontally. A fixture, e.g. a thin pipette, keeps the drop in place allowing high resolution imaging of the advancing and receding part of the sliding drop. Simultaneously, the fixture can be a force sensor and measuring the lateral force directly. In a device called “drop adhesion force instrument”, the lateral force is measured by means of a deflectable capillary stuck in the sessile drop or a captive bubble (Fig. 4E) [31, 62, 80-83]. The advantage of this setup is that force is measured when the substrate is moved at a controlled speed. At the same time, a camera in side view images the advancing and receding sides of the drop to determine the contact angles.

The propagation of wall-bound drops on a solid substrate can also be driven by aerodynamic forces induced by a gas flow (Fig. 4F). This phenomenon is usually studied for better understanding of the mechanisms leading to the ice accretion on aircraft surfaces or modeling of water flow on car surfaces. This phenomenon is less used as a measurement method for the contact angle dynamics since it requires a special equipment, including a well-calibrated wind tunnel with an optical access. The difficulties are also caused by some uncertainties in the estimation of the aerodynamic forces. On the other hand, these experiments allow to characterize the behavior of the propagating contact lines of the drop under complicated oscillatory motion and in the presence of the aerodynamic stresses.

In wind tunnel experiments the drop geometry during propagation is usually observed by a high-speed video camera. Both, advancing and receding contact angles can be measured in such experiments. Moreover, the evolution of both angles in time and as a function of the drop average propagation velocity can be accurately determined. The condition of the

inception of the drop propagation is determined by the balance of the adhesion force F_c (eq. 2) and the aerodynamic force, which is modeled in the form [84-87]

$$F_a = c_D \rho_{gas} U_{attack}^2 A, \quad (4)$$

Here, c_D is the drag coefficient, ρ_{gas} is the gas density, A is the projected cross-sectional drop area, exposed to the flow and U_{attack} is the "attack" velocity of the gas flow, that is the velocity of the gas flow at the drop half height. If the drop height is much larger than the thickness of the viscous boundary layer the attack velocity can be approximated by an average gas velocity in the channel.

If the aerodynamic force exceeds the lateral adhesion force, the drop starts to propagate with a certain velocity, which increases for high gas speed. The dynamics of the drop motion is mainly influenced by viscous forces appearing in the vicinity of the contact line and in the drop tail [88]. Often, the movement of drops under hydrodynamic drag is not smooth, continuous and steady but periodically changing [83]. In some cases, drop oscillations are observed, especially at low capillary numbers. If oscillations of the propagating drop are significant, the values of the apparent contact angles also fluctuate in time. Moreover, an apparent stick-slip motion of the advancing and receding contact lines is often observed. This stick-slip motion and other transient effects in the neighborhood of the contact line are not yet completely understood and require further investigation.

5. Effects leading to contact angle hysteresis

Two effects have been identified early on as contributions to contact angle hysteresis: Heterogeneity and roughness (or surface structure) [5, 7, 23, 52, 89, 90]. Meanwhile it is clear that in addition, the deformation of the substrate by the contact line and adaptation also lead to contact angle hysteresis (Fig. 5). In a strict sense, both effects only lead to contact angle hysteresis when the contact line is moving. In many applications even very slow motion is effective so that practically one has to consider deformation and adaptation even in the static case.

Heterogeneity and roughness

A heterogeneous solid surface consists of patches with different surface chemistry or molecular structure leading to local variations in the solid surface energies. For the equilibrium contact angle the Cassie-Baxter formalism is accepted to lead to the correct value of Θ_e [91-93]. An underlying assumption is that the radius of curvature of the contact line is much larger than the typical size and spacing of surface features. Unfortunately, no simple equation exists to calculate the influence of heterogeneity on contact angle hysteresis. A simple average over the disorder is not sufficient to predict the details of contact angle hysteresis but the detailed structure needs to be considered [37, 94]. The progression of the contact line on heterogeneous surfaces consists of sticking, stretching, and jumping events along the patches

[35, 95]. At the borders of these patches the free energy is at a local minimum and hence the contact line can remain in several metastable states [52, 92, 94].

Several theoretical [35, 37, 52, 92, 94, 96] and experimental [95, 97-99] studies have addressed the problem. The critical energy needed to move the contact line, i.e. to overcome the energy barriers between the heterogeneous patches, depends on the shape and size of the patches. For example, for a drop moving perpendicular to stripes, hysteresis can be high while for a movement in parallel direction hysteresis is low. Typically, the movement of the contact line is slower on heterogeneous surfaces compared to homogeneous surfaces due to the pinning and depinning events and hence heterogeneous surfaces can be used to control the wetting speed [95]. In recent experiments with checkerboard micropatterned surfaces, Becher-Nienhaus et al. studied the influence of pattern size on contact angle hysteresis [99]. If both regions themselves have a similar contact angles hysteresis, the pattern size did not have a significant influence on the apparent contact angle hysteresis. If, however, contact angle hysteresis on the individual surface was different, the apparent contact angle hysteresis increases with pattern size.

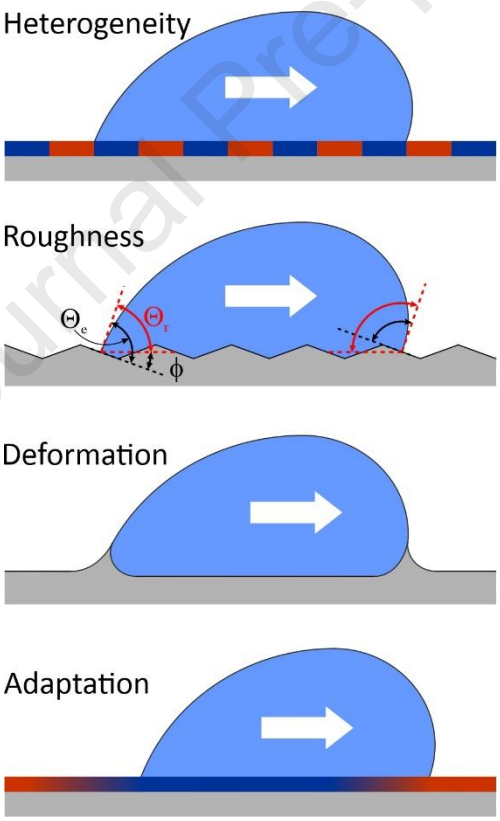

***Figure 5**. Different effects leading to contact angle hysteresis.*

In contrast to liquids, solids are usually rough. They are covered by microgrooves and striations from fabrication or aging. Flat and smooth surfaces over macroscopic length scales are more an exception. Examples are float glass produced on molten metal, freshly cleaved Mica or annealed polymer films. Adam [100], Wenzel [101], Cassie and Baxter [91] have as one of the

first studied the influence of roughness on equilibrium contact angles [93]. In addition, roughness can lead to contact angles hysteresis because the local slope on a surface may deviate from the apparent slope (Fig. 5). Locally, on the microscopic scale, Young's equation may still be followed [20]. For a surface which due to roughness has a maximal slope ϕ the apparent advancing and receding contact angles would be given by $\Theta_a = \Theta_e + \phi$ and $\Theta_r = \Theta_e - \phi$ [33, 102, 103]. Contact angle measurements of rough and porous surfaces have been reported and demonstrate this behaviour of the contact angle hysteresis [52, 104, 105]. As for heterogeneous surfaces, the degree of contact angle hysteresis depends on the specific structure and direction of motion [90, 106]. It is impossible to give general trends or report simple general equations.

In many respects rough patches or patches with different surface energy bear similarities. Both can be viewed as pinning centers. The strength of the pinning center depends on the size and shape [20] or the size and surface energy of the patch [107]. On a length scale much larger than the size of the pinning center, both have a similar effect. Therefore, significant effort has been devoted to better understand the effect of pinning centers. That pinning centers exist on many surfaces is supported by the observation that contact lines do not move continuously but that locally they move in a stick-slip motion [51]. In this context, several questions arise: How does the strength, size and distribution of pinning centres lead to contact angle hysteresis [108]? How does a single defect deform the contact line [107]? How is the motion of contact lines influenced by pinning centers [109-111]?

One illustrative approach is to consider the effect of defects on two-dimensional drops; thus drops with a cylindrical shape and stripes as defects oriented perpendicular to the motion of the drops. By solving the Navier–Stokes equation, Thiele and Knobloch could obtain a phase diagram of pinning/depinning for a drop by a hydrophobic/hydrophilic patch [112]. Depending on the driving forces, a ''hydrophobic'' defect blocks the drop in front and a ''hydrophilic'' one holds it at the back at the rear. Park and Kumar focussed more on topological defects [113]. They reported that the critical pinning occurs at the location of the minimum slope (i.e., maximum defect angle) of a topographical defect.

Pinning of three-dimensional drops was treated by Joanny and de Gennes [107], who proposed a model to describe the effect of a single defect and then extended this model to a distribution of defects. For a single defect of size d which exerts a total force f on the contact line they analyzed the perturbation of the contact line and the shape of the liquid surface. In their formalism it does not matter if the force is caused by inhomogeneity of the surface or by structural features. As a first order they find a linear relation (Hookean elasticity) between the maximum displacement of the contact line δ and the force:

$$\delta = \frac{f}{\pi\gamma_L(\tan\theta)^2}\ln\frac{L_{pc}}{d} \tag{5}$$

Here, L_{pc} is a maximal cutoff length, which is practically e.g. the width of the contract area of a sessile drop. The contact angle of the liquid on the substrate surrounding the defect Θ is

assumed to be below 90°. Once a certain threshold has been overcome the contact line passes the pinning site, is released and the work carried out to stretch it is dissipated as heat.

The proposed elastic behavior of the contact line and its calculated shape was experimentally confirmed [114, 115]. Based on the model of Joanny and de Gennes, Reyssat and Quere [110] considered the contact angle hysteresis expected for an array of pinning sites. Experimentally they realized it by making arrays of micropillars, where each top face of a micropillar is a pinning site of defined size. One can relate the horizontal force on the contact line per unit length to the typical energy barrier between pinning sites E^* and the mean distance between pinning sites λ by $\gamma_L(\cos\Theta_r - \cos\Theta_a) \approx E^*/\lambda^2$ [56, 111, 116].

Flexible and soft surfaces

One derivation of Young equation uses a balancing of the lateral forces arising from the interfacial tensions at the contact line. However, there is also an additional vertical component of the liquids surface tensional force that leads to a vertical displacement of the solid substrate. The magnitude of this deformation is on the order of the so-called elastocapillary length. It is defined as the ratio between liquid surface tension and elastic modulus of the solid, $l_c = \gamma_L/E$. For hard solids, the elastocapillary length is of the order of atomic distances and therefore the deformation of the solid can be neglected. For soft solids, such as elastomers with low crosslinking density or hydrogels, the elastocapillary length can be in the order of micrometers. On such soft solids, the vertical component of surface tension leads to the formation of a wetting ridge. In addition, the Laplace pressure in the drop leads to a depression of material underneath the drop. The resulting wetting ridge shape has been visualized in situ by white light interferometry [117], confocal microscopy [118], X-ray microscopy [119] or direct optical video imaging with backlight illumination [120]. Early models to describe the wetting ridge based on linear elastic theory were introduced by Lester [17], de Gennes and Shanahan [121] and Rusanov [122]. For droplet sizes much larger than the elastocapillary length, the apparent macroscopic contact angle is essentially equal to the Young contact angle, while the microscopic contact angle is given by the Neumann triangle [123]. For small droplets, with diameters approaching the elastocapillary length, contact angles will become smaller than predicted by the Young equation and approach the ones predicted by the Neumann equation. This implies also, that for small droplets, a gradient in the substrate stiffness can lead to differences in the (equilibrium) contact angle and thus to a net driving force on the droplet. It was indeed observed that such gradients can lead to "durotaxis" of small droplets [124].

The existence of the wetting ridge with a sharp cusp might lead to pinning of the contact line and thus an increase in contact angle hysteresis. A simple model relating contact angle hysteresis to ridge size was introduced by Extrand and Kumagai [125]. Based on simple geometric considerations they predicted changes in the advancing and receding contact angles of the order of $\Theta_a \approx \Theta_{a0} + \frac{6\gamma_L}{bE}\sin\Theta_{a0}$ and $\Theta_r \approx \Theta_{r0} - \frac{6\gamma_L}{bE}\sin\Theta_{r0}$, where Θ_{a0} and Θ_{r0}

are the advancing and receding contact angles on the undeformed surface. b is the half-width of the wetting ridge, which was approximated by a symmetric triangle with height given by the de Gennes model. They experimentally observed increase of contact angle hysteresis with decreasing elastic modulus of elastomers with $E < 5$ MPa. A comparison of their experimental results with the model was not possible as ridge dimensions were too small to be directly observed. This model was later extended for the case of straight contact lines [126].

The models mentioned so far were all based on linear elastic response of the materials. In practice, however, soft materials will show viscoelastic behaviour when subjected to cyclic loads. The movement of the contact line with a wetting ridge over a soft viscoelastic material will lead to a local strain cycling of the material with significant viscous dissipation. This "viscoelastic breaking" can lead to significant slowdown of the spreading of droplets [117]. Also droplets running down an inclined plane experience this viscoelastic breaking [127]. As a consequence, the sliding speed of the droplets on soft polymers is determined by the rheology of the polymer. Viscous dissipation at the wetting ridge becomes dominant compared to viscous dissipation within the droplet itself. This coupling between contact line motion and rheology of the underlying polymer can lead to complex dependence of contact angles on contact line velocity, including stick-slip motion [128, 129], which may be related to a strain rate dependent surface tension of the solid [120]. However, also a non-linear elastic response of the substrate could be a possible explanation [130]. Recent studies on contact line dynamics have included a possible strain dependence of the solid surface tension (Shuttleworth effect) [131]. It was found that the Neumann law is still fulfilled for the microscopic contact line [132]. However, an additional rotation of the solid ridge occurs. This dynamic change in tilt of the solid cusp was found to scale with a power law, which is given by the power law dependence of the loss modulus of the polymer substrate.

Adaptation

Early on scientists adopted the concept that the solid somehow adapts to the presence of the liquid or its vapour [133]. This would leave a more wettable surface when the receding angle is measured. As a results, the interfacial tension γ_S and γ_{SL} on the front side of a moving drop and on its rear side may be different. Johnson & Dettre [52] and Andrade et al. [5] even distinguish two classes of hysteresis: *True* or *thermodynamic* hysteresis, where the hysteresis curve is reproducible over many cycles and independent of time or frequency and *kinetic* hysteresis, where the curves changes with time or frequency. The second class of curves is usually correlated with adaptation. Many polymers reconstruct due to a reorientation of side groups, a selective exposure of specific segments or the diffusion of liquid into the polymer [53-55, 64-66, 68, 134-139]. Liquid can diffuse into polymers or monolayers [63]. If the amount of liquid diffusing into the polymer is significant and polymer and liquid are partially miscible, the polymer will swell [64, 140, 141]. Water, for example, swells polyethylene glycol (PEG) or polyelectrolyte brushes [138]. Surfaces have even deliberately coated with mixed polymer brushes which change their structure depending on the type of fluid they are exposed to [140,

142-148]. One may also consider the replacement of a contamination/adsorption layer as an adaptive process. As soon as a surface is exposed to air, water and airborne hydrocarbons adsorb. When the surface is wetted, the adsorbed layer changes its structure, is replaced, or dissolves.

Hansen & Miotto [149] and later Elliott & Riddiford [150] pointed out that, in the liquid, molecules adapt to the presence of the solid and change their structure close to the interface. This would lead to a time dependent change in γ_L and thus to a change in the contact angle. The liquid also "adapts" to the presence of the solid interface and thus a change in γ_{SL}. For water molecules, reorientation is fast and equilibrium of the liquid structure is established in ≈10 ps so that contact angles are not affected. Other processes may however have an effect, such as the adsorption of surfactant [151-155] or the formation of electric double layers.

For perfectly reversible processes, adaptation should not affect the static contact angle hysteresis. However, practically all measurements of contact angle hysteresis are not infinitely slow. To estimate if contact angle measurements are influenced by adaptation some of us suggested a simple criterion [156]. Assuming that the adaptation of the solid-liquid interface takes a characteristic relaxation time τ_{SL}, the effect on the dynamic contact angle is negligible for $U \ll l/\tau_{SL}$. Here, U is the velocity of the contact line and l is the so called "peripheral thickness". We define the peripheral thickness as the width of the region around a contact line, which influences the contact angle [149, 156]. It depends on the specific contact angles and the materials used. We suggest that l = 10-100 nm is a reasonable value. For example, if the relaxation of a polymer takes τ_{SL}=2 ms and we assume l=0.1 µm, adaptation is only negligible for speeds of the contact line much lower than 50 µm/s [68]. This speed is slower than the one used in most measurements and thus adaptation would lead to apparent contact angle hysteresis.

Irreversible interaction

Makkonen suggests another fundamental effect leading to contact angle hysteresis [10]. He argues that when a contact line recedes, free solid surface is created behind the contact line. The corresponding work, according to Makkonen, is not regained and dissipates as heat. This leads to unavoidably friction of the contact line and thus contact angle hysteresis.

Any process dissipating energy at the front of a moving drop which is not regained at the rear should lead to contact angles hysteresis. We still believe, that the argument cannot be used as a fundamental criticism to Young's equation. We think that the work carried out to create free solid surface can in principle be regained, unless there are other irreversible dissipative processes. Let us therefore, like Makonnen, consider a drop sliding down a tilted plate. At the rear, free solid surface is created and the work $dE = w(\gamma_S - \gamma_{SL})dx$ is carried out by the drop (Fig. 6A). The same work is, however, gained at the front. Both are coupled by the surface tension across the liquid drop.

We can also consider an infinitesimal shift of the contact line. Then, any change in solid-liquid interfacial area $dA_{SL} = -dA_S$ is accompanied by a change in surface area of the liquid dA_L. If the contact angle is at its thermodynamic equilibrium, the changes in surface area weighted with their respective interfacial energies would compensate: $(\gamma_S - \gamma_{SL})dA_{SL} = \gamma_L dA_L$. Thus any creation of free solid surface is accompanied also with a gain in free energy of the liquid surface. As an example let us consider a drop with contact radius a, radius R and height h on a flat surface (Fig. 6B). Its volume is assumed to be constant, $dV_L = 0$. Neglecting gravity and assuming that the drop is shaped like a spherical cap $dV_L = \pi ahda + \pi hRdh \Rightarrow \pi hdh = -\frac{\pi ah}{R}da$. When shifting the contact line outward by da, the energy $(\gamma_S - \gamma_{SL})dA_{SL} = 2\pi a(\gamma_S - \gamma_{SL})da$ is lost (gained). However, when the contact angles is equal to the Young angle the same energy is gained (lost) by the free liquid surface; it is not necessarily dissipated by heat. To demonstrate this argument, one can consider the change in liquid surface area. With $A_L = \pi(a^2 + h^2)$ it is $\mathrm{d}A_L = 2\pi ada + 2\pi hdh = 2\pi ada - 2\pi a\frac{h}{R}da$ or $dA_L = 2\pi a\left(1 - \frac{h}{R}\right)da = 2\pi a\cos\Theta\, da$. The last step was again for geometric reasons. Multiplying this expression with γ_L directly shows that both energies are equal, if Θ is the Young contact angle: $2\pi a(\gamma_S - \gamma_{SL})da = 2\pi a\gamma_L\cos\Theta\, da$.

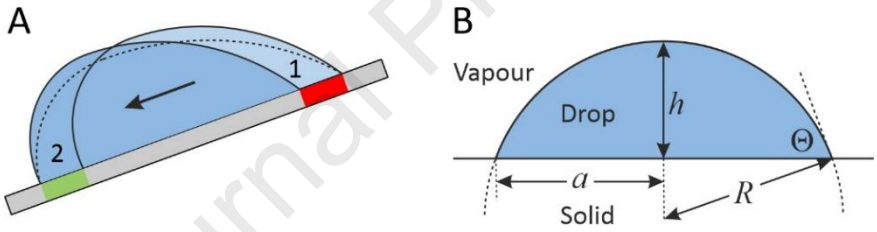

***Figure 6**. (A) When a drop slides down an inclined plane free solid surface disappears and solid-liquid interface is created at the front. At the rear, free solid surface is formed while solid-liquid interface disappears. We argue that both processes are coupled so that the work accompanied the two processes does not need to dissipate as heat. (B) Schematic of a sessile drop.*

6. Dynamic contact angle hysteresis

When the contact line is moving, the contact angles depend on the velocity [131, 151, 157]. The advancing contact angle increases, the receding contact angle decreases with increasing velocity (Fig. 7). Dynamic contact angle hysteresis is the difference of the advancing contact angle and the receding contact angle for a contact line moving in an opposite direction at the same velocity [29].

Roughness and heterogeneities not only lead to a static contact angle hysteresis. They also influence dynamic contact angles [158, 159]. Pinning sites temporarily hinder the contact line to move. Energy is temporarily stored in the local stretching of the contact line. When the tension on the contact line at that site exceeds a certain threshold, the contact line is released

[72, 107, 111]. The work put into locally stretching the contact line dissipates as heat. For a distribution of pinning sites, this effect leads to a speed dependence of the apparent advancing and receding contact angles.

For deformable surface, viscoelastic processes in the solid dissipate energy. Adaptation is another reasons for energy dissipation and a change in the apparent contact angles. In the case of adaptation the energy "loss" is due to spontaneous change of the interfaces outside the core region. For example, when a drops slides over an adaptive surface, right behind the front contact line the solid-liquid interfacial energy is $\gamma_{SL}{}^0$. The longer the surface is in contact with the liquid the more it adapts and the interfacial energy decreases spontaneously to $\gamma_{SL}^{\infty} = \gamma_{SL}^0 - \Delta\gamma_{SL}$. If this adaptation is slow compared to l/U, the contact angle on the advancing side is given by $\cos\Theta_a = (\gamma_S - \gamma_{SL}^0)/\gamma_L$. Let us further assume that the surface has sufficient time to fully adapt, while it is in contact with the liquid. Then, at the receding side the contact angle is given by $\cos\Theta_r = (\gamma_S - \gamma_{SL}^{\infty})/\gamma_L$. Thus, in order to move a drop of width w a force $F_c \approx w(\gamma_{SL}^0 - \gamma_{SL}^{\infty})$ is required leading to a power dissipation of $P_c \approx wU(\gamma_{SL}^0 - \gamma_{SL}^{\infty})$. For single adaptation process which are assumed to follow first order kinetics the expected dynamic contact angles are [156]

$$\cos\Theta_a\,(U) = \cos\Theta_a^0 - \frac{\Delta\gamma_{SL}}{\gamma_L} e^{-l/U\tau_{SL}} \text{ and } \cos\Theta_r\,(U) = \cos\Theta_r^0 + \frac{\Delta\gamma_S}{\gamma_L} e^{-l/U\tau_S} \quad (6)$$

Here, we assumed the liquid surface relaxes fast, which for water is a realistic assumption. τ_{SL} and τ_S are the characteristic relaxation times for the adaption of the surface when getting into contact with the liquid and when becoming dry again. The strengths of the respective adaptation processes are quantified by $\Delta\gamma_{SL}$ and $\Delta\gamma_S$, respectively.

Overcoming energy barriers

Traditionally, dynamic changes in contact angles are attributed either to thermally activated processes on the molecular scale [160, 161], that is, the contact line has to overcome local microscopic or atomic energy barriers, or to hydrodynamic viscous dissipation [58, 89, 162, 163].

On the molecular scale and driven by thermal fluctuations liquid molecules near the contact line are jumping from the liquid phase to binding sites on the solid surface or they are jumping from one binding site to the next overcoming energy barriers of the order of k_BT. k_B is Boltzmann's constant and T is temperature [56]. Thus, the movement of the contact line is a collective thermal motion of liquid molecules under the influence of the capillary driving force. The capillary driving force is $\gamma_L(\cos\Theta_e - \cos\Theta_d)$. If the actual dynamic contact angle Θ_d is larger than Θ_e, more liquid molecules move forward and the liquid front advances. For $\Theta_d < \Theta_e$ more liquid molecules jump from the surface region into the liquid and the liquid front recedes. This idea has led to the molecular kinetic theory (MKT), which describes dynamic contact angles as a result of molecular adsorption and desorption processes at the moving

contact line [59, 61, 89, 160]. According to this molecular kinetic theory the dynamic contact angles are related to velocity by

$$\cos\Theta_{a/r}(U) = \cos\Theta^0_{a/r} - \frac{2k_BT}{\gamma_L\lambda^2}\sinh^{-1}\left(\frac{U}{2\kappa\lambda}\right) \quad (7)$$

Here, the constant $1/\lambda^2$ is the number of interaction sites per unit area on the solid surface and κ is the equilibrium frequency of the random molecular displacements occurring within the three-phase zone. Typical values are λ=1 nm and κ=10 GHz. Eq. (7) can be applied for advancing and receding contact angles [61, 89]. U is counted positive on the advancing and negative on the receding side. The theory has been applied in general to processes which are expected to involve the jump of the contact line over energy barriers by thermal fluctuations [56, 57, 164, 165].

Hydrodynamic dissipation

Another reason for contact angles to change with speed is hydrodynamic dissipation [75, 166-172]. Viscous forces arise because of viscous hydrodynamic flow within the drop. Calculating the flow inside a drop with the Navier-Stokes equations sounds straight-forward (at least for laminar flow). However, the problem is that continuum hydrodynamic theory leads to divergent stress fields at the contact line. It also turned out that viscous dissipation close to the contact line dominates [71, 75, 173] and that bulk viscous dissipation for water is usually negligible. This problem of a divergent stress field has been solved by the assuming that close to the contact line, in a region described by the microscopic length L_m, the usual no-slip boundary condition at the solid-liquid interface is relaxed and slip is allowed [167, 174-177]. Thus, two length scales are relevant: The outer region L (>>10 µm), where the apparent contact angle is measured, and the inner region where surface effects, such as slip, are allowed. For many surfaces, a molecular length scale is applied, e.g. L_m=1 nm [178-180]. Since we observe contact angles at a larger length scale, viscous dissipation in the wedge would manifest itself in a change of the macroscopic contact angles. How the macroscopic contact angles depend on the speed has been calculated by Cox and Voinov [167, 171, 181]:

$$\Theta^3_{a/r}(U) = \left(\Theta^0_{a/r}\right)^3 + \frac{9\eta U}{\gamma_L}\ln\frac{L}{L_m} \quad (8)$$

Here, the angles are given in rad. For the outer region often the capillary length, L=2.7 mm for water, is taken.

Unfortunately, neither the MKT nor the hydrodynamic theory are a priori predictive. They still contain the parameters L/L_m or λ and κ. These parameters are determined by a curve fitting of experimental data.

As a rule of thumb, hydrodynamic energy dissipation is important at high capillary numbers, but can be neglected below typically $|Ca|$ ≈0.001-0.005, which for water is few 10 cm/s [60, 182] (Fig. 7). To describe the often observed changes in $\Theta_r(U)$ and $\Theta_a(U)$ at low velocity, some authors combined MKT and hydrodynamic theories [183-185]. They replace the static

advancing and receding contact angles $\Theta_a{}^0$ and $\Theta_r{}^0$ in Eq. (8) with the microscopic, static advancing $\Theta_{ma}{}^0$ and receding $\Theta_{mr}{}^0$ contact angles which the obtain with Eq. (7). In this way, viscous dissipation in the inner region *and* energy dissipation at the contact line by thermally activated processes are taken into account. Petrov & Petrov suggested such a combination [89, 186]:

$$\Theta_{a/r}^3(U) = \left(\Theta_{ma/r}^0\right)^3 + \frac{9\eta U}{\gamma_L}\ln\frac{L}{L_m} \qquad \text{with} \tag{9}$$

$$\cos\Theta_{ma/r}(U) = \cos\Theta_{a/r}^0 - \frac{2k_BT}{\gamma_L\lambda^2}\ln\left[\frac{U}{2\kappa\lambda} + \sqrt{\left(\frac{U}{2\kappa\lambda}\right)^2 + 1}\right]$$

Here, we used the identity $\sinh^{-1} x = \ln\left(x + \sqrt{x^2+1}\right)$. The validity of Eq. (9) has been nicely verified by recent molecular dynamics simulations [182]. They found excellent agreement for L/L_m = 2.1. Hydrodynamic theory alone fitted the simulations best with $L/L_m \approx 8$.

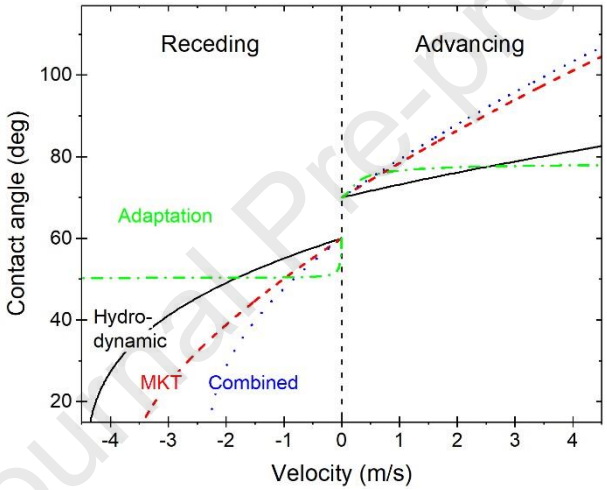

Figure 7. *Dynamic contact angles calculated for static contact angles $\Theta_a{}^0$=70°and $\Theta_r{}^0$=60° with hydrodynamic theory (eq. 8 with L/L_m = 8, black), MKT theory (eq. 7 with κ=8.6 GHz, λ=0.36 nm, red), the combined MKT & hydrodynamic theory (eq. 9 with L/L_m = 2.1, κ=8.6 GHz, λ=0.36 nm, blue) and adaptation theory (eq. 6, τ_{SL}=0.5 µs, τ_S=10 µs, $\Delta\gamma_{SL} = \Delta\gamma_S$ =0.1 N/m, l=100 nm, green) for water (η = 0.001 Pa s, γ_L = 0.072 N/m). The parameters were motivated by experiments on PET (Polyethelene terephthalate) and computer simulations for the hydrodynamic, MKT and combined theory [89, 182] and by experimental results on a styrene-acrylic acid copolymer [68].*

To describe contact angles at lower speed, MKT is required and adaptation or viscoelastic dissipation in the substrate play a role.

7. Surfaces with low contact angle hysteresis and super liquid-repellent surfaces

Flexible polymer brushes

To increase the receding contact angle and reduce the contact angle hysteresis on smooth surfaces is a huge challenge. Proper control of both the molecular architecture and the physical nature of the surfaces are required [187]. An emerging category of surface which is composed of flexible polymer (polyethylene glycol, polydimethylsiloxane, and perfluorinated polyether, etc.) brushes brings a simple and effective possibility to reduce the lateral adhesion of liquids [188-191] (Fig. 8A). Resulting from the high mobility of the main chain in these surface-tethered molecules, the surfaces exhibit a liquid-like lubricating effect to drops with contact angle hysteresis for both water and low-surface-tension liquids including hexane (surface tension: 18.4 mN/m) being lower than 5˚ [188, 192, 193]. Specifically, surfaces coated with polydimethylsiloxane (PDMS) brushes exhibit excellent resistance to high-temperature treatment, photodegradation, and even scratching [30, 188, 193-195]. In addition, since the layers are only a few nanometers thick, they are transparent, do not influence the appearance of coated surfaces.

One should be aware that often PDMS brushes still contain oligomers, which can further reduce the liquids' contact angle hysteresis. One may even deliberately add a lubricant. Lubricant can be any second liquid which mixes with the brush but not with the liquid in the drop (Fig. 8B) [196]. However, with time these oligomers are washed out and the contact angle gradually becomes that of the pure brush [195].

Lubricant-impregnated surfaces

Drops also easily slide off lubricant-impregnated surfaces [82, 197-200] (Fig. 8C). Therefore, they are also called SLIPS (slippery lubricant-infused surfaces). Here, a porous surface is impregnated with a lubricant. The lubricant wets the porous surface but is immiscible with the liquid. The concept was first proposed by David Quéré [201]. Quéré assumed that the lubricant fills the pores whereas the tops of the porous surface remain dry. A deposited drop partially rests on the top faces of the underlying microstructure and partially on lubricant. The mobile liquid layer greatly reduces contact line pinning [197, 202]. As mentioned above, a variant of lubricant-impregnated surfaces are organogels or polymer brushes, which contain a chemically compatible lubricant, e.g. PDMS brushes with silicon oil and with water as a liquid [67, 82, 203, 204] (Fig. 8B).

A limit for lubricant-infused surfaces is that sliding drops can take lubricant along. The lubricant depletes. To slow down lubricant depletion, as liquid lubricant typically silicone oil, mineral oil or a fluorinated oil are used [205]. These lubricants have in common that the viscosity can be varied by a few orders of magnitude. The viscosity of the lubricant influences the shear stress at the mobile lubricant drop interface [206, 207]. High viscous lubricants

deplete slower. Silicone oil and fluorinated oils also have the advantage that they are hardly soluble in aqueous or hydrocarbon based liquids. Depletion of lubricant by diffusion into the liquid drop can be neglected.

With respect to contact angle hysteresis and friction, the following two aspects discriminate drops on lubricated surfaces from drops on solid surfaces. (i) On a lubricated surface, a drop is surrounded by a wetting ridge [202]. The wetting ridge forms because the surface tension of the liquid pulls the lubricant upwards. The wetting ridge poses a challenge for the measurement of the advancing and receding contact angles [199, 208]. Most optical methods cannot distinguish between the drop and the lubricant. Therefore, the real three phase contact line is hidden. Furthermore, most lubricants cloak aqueous drops [202]. This challenges the concept of the definition of a three phase contact line. To circumvent these problems, an apparent contact angle and an apparent contact angle hysteresis has been defined [200]. Although, these values describe pinning strength of drops on lubricant impregnated surfaces reasonably well, the contact angles can greatly differ from those measured by confocal [199, 208, 209] or x-ray microscopy [119].

(ii) Lubricant-impregnated surfaces are known for their low pinning strength. Although pinning is negligible, sliding friction can be large. This stimulated research on the origin of friction on lubricated surfaces. In contrast to Eqs. 2 and 3, on lubricated surfaces friction is dominated by viscous dissipation in the wetting ridge [206, 207, 210].

Thus, the concepts which determine contact angles and contact angle hysteresis on lubricant impregnated surfaces significantly differ from those on solid surfaces. Therefore, we focus on drops on solid surfaces in contact with air in the remaining part of this review.

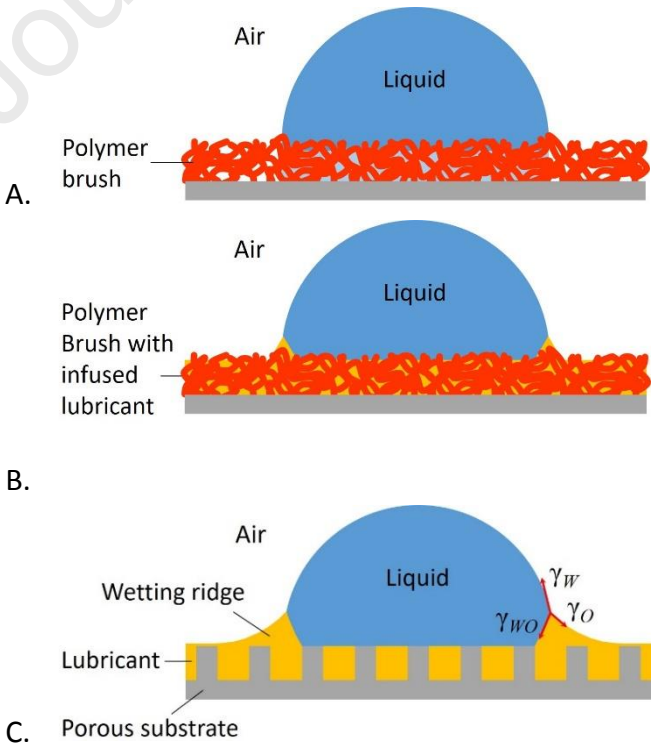

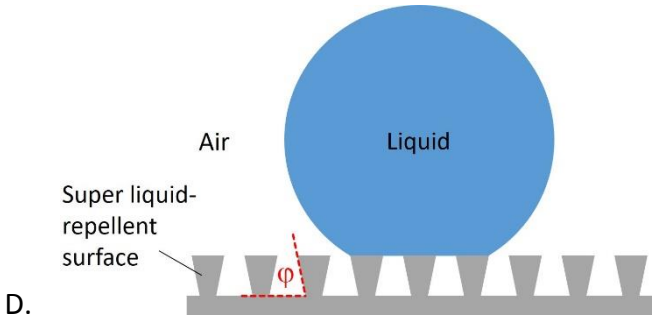

***Figure 8**: (A) A liquid drop placed on a flexible polymer-coated surface. (B) To further reduce contact angle hystereis, a lubricant may be added (orange). (C) A liquid drop placed onto a lubricant-impregnated micropillar array. The drop is surrounded by a wetting ridge. In this example we took water as the liquid and an oil as lubricant. We assumed that the oil does not cloak the water but that it forms defined Neumann angles given by the surface tension of water, γ_W, the surface tension of the oil, γ_O, and the interfacial tension water-oil, γ_{WO}. (D) Liquid drop on a super liquid repellent surface.*

Super liquid-repellent surfaces

A special case of "roughness" are deliberately structured surfaces, in particular super-liquid repellent surfaces. Superhydrophobic (water repellent) or superoleophobic (oil repellent) surfaces have high apparent receding contact angles, typically higher than 140° [72, 73, 103, 105, 110, 111] (Fig. 8D). This is achieved by nano- and microscopic protrusions with steep side walls. The slope of the side walls φ has to be lower than the advancing contact angle Θ_a on a flat, smooth surface of the same material, $\varphi < \Theta_a$ [211-214]. Thus, for superhydrophobic surfaces usually a slope of 90° is sufficient because many materials have Θ_a>90°. However, for oil-repellent surfaces, overhanging structures with φ<90° are required because oils do not form such high contact angles, not even on fluorinated surfaces [215, 216].

Often it is assumed that on super-liquid repellent surface the contact angle hysteresis is low because drops easily roll off; roll-off angles are typically below 10°. According to Eq. (3) one may thing that a low roll-off angle is correlated with a low contact angle hysteresis. This, however, is not the case. In contrast, for superhydrophobic arrays of micropillars it could be demonstrated that the apparent advancing contact angle is Θ_a^{app}≈180° [217]. Thus, for typical apparent receding contact angles of Θ_r^{app}=150° the hysteresis is 30°. Drops roll off easily because of two reasons. First, the contact width w is low. Second, for angles around 180° the cosine does not change so much anymore. Thus, as long as Θ_r is high, the precise value of Θ_a is not critical anymore.

8. Summary

Static contact angle hysteresis is caused by roughness and heterogeneity. Surface features lead to pinning of the contact line and thus to an increase of the apparent advancing and a

decrease of the apparent receding contact angle. In addition, surface adaptation and deformation can lead to changes in apparent contact angles. They depend on the characteristic time of the adaptation process or the specific viscoelastic properties of the surface material. In a strict sense, adaptation and elastic deformation are time dependent. Practically, they can be so slow that they are perceived as static changes in contact angle. Pinning, adaptation and viscoeleastic deformation of the surface lead to a velocity dependence of the apparent advancing and receding contact angles. Dynamic contact angles occur even on atomically smooth surface due to thermally activated processes at the atomic scale and, at velocities around or above 1 m/s, due to hydrodynamic dissipation. Thus, contact angle hysteresis is caused by phenomena at the micro-, nano-, or even atomic scale. Unless another component, a lubricant, is introduced, contact angle hysteresis is unavoidable. Being able to control contact angle hysteresis is an important challenge for surface engineering, because it provides friction to moving contact lines.

9. Acknowledgements

This project has received funding from the European Research Council (ERC) under the European Union's Horizon 2020 research and innovation programme (Advanced grant DyanMo, No 883631). The authors further acknowledge financial support by the German Research Foundation (DFG) with the Collaborative Research Center 1194 (H.-J.B., R.B.), the Priority Programme 2171 (D.V., R.B., H.-J. B.) and the European Union's Horizon 2020 research and innovation program LubISS No. 722497 (D.V.).

10. Reference

[1] Young T. An essay on the cohesion of fluids. Phil. Trans. Roy. Soc. London 1805; 95:65-87.

[2] Gibbs JW. The Collected Works of J. Willard Gibbs, Thermodynamics. New Haven: Yale University Press; 1928.

[3] White LR. On deviations from Young's equation. J. Chem. Soc., Faraday Trans. I 1977; 73:390-398.

[4] de Gennes PG. Wetting: Statics and dynamics. Rev. Modern Phys. 1985; 57:827-863.

[5] Andrade JD, Smith LM, Gregonis DE. The contact angles and interface energetics. In: Surface and Interfacial Aspects of Biomedical Polymers. Andrade JD (Editor) New York & London: Plenum Press; 1985. pp. 249-292.

[6] Rusanov AI. Thermodynamics of solid surfaces. Surface Science Reports 1996; 23:173-247.

[7] Marmur A. Solid-surface characterization by wetting. In: Annual Review of Materials Research. 2009. pp. 473-489.

[8] Quincke G. Ueber den Randwinkel und die Ausbreitung von Flüssigkeiten auf festen Körpern. Annalen der Physik und Chemie, Neue Folge 1877; 2:145-195.

[9] Kralchevsky PA, Danov KD, Kolev VL, Gurkov TD, Temelska MI, Brenn G. Detachment of oil drops from solid surfaces in surfactant solutions: Molecular mechanisms at a moving contact line. Ind. Eng. Chem. Res. 2005; 44:1309-1321.

[10] Makkonen L. A thermodynamic model of contact angle hysteresis. J. Chem. Phys. 2017; 147:064703.* He presents a universal model to explain contact angle hysteresis even on ideal solid surfaces.

[11] Das SK, Binder K. Does Young's equation hold on the nanoscale? A Monte Carlo test for the binary Lennard-Jones fluid. Europhys. Lett. 2010; 92:26006.

[12] Hautman J, Klein ML. Microscopic wetting phenomena. Phys. Rev. Lett. 1991; 67:1763-1766.

[13] Seveno D, Blake TD, De Coninck J. Young's equation at the nanoscale. Phys. Rev. Lett. 2013; 111:096101.

[14] Tretyakov N, Mueller M, Todorova D, Thiele U. Parameter passing between molecular dynamics and continuum models for droplets on solid substrates: The static case. J. Chem. Phys. 2013; 138:064905.

[15] Wayner PC. The interfacial profile in the contact line region and the Young-Dupré equation. J. Colloid Interface Sci. 1982; 88:294-295.

[16] Churaev NV, Starov VM, Derjaguin BV. The shape of the transition zone between a thin film and bulk liquid and the line tension. J. Colloid Interface Sci. 1982; 89:16-24.

[17] Lester GR. Contact angle of liquids at deformable solid surfaces. J. Colloid Sci. 1961; 16:315-326.

[18] Decker EL, Frank B, Suo Y, Garoff S. Physics of contact angle measurement. Colloids & Surfaces A 1999; 156:177-189.

[19] Semprebon C, Herminghaus S, Brinkmann M. Advancing modes on regularly patterned substrates. Soft Matter 2012; 8:6301-6309.

[20] Jansons KM. Moving contact lines on a two-dimensional rough surface. J. Fluid Mech. 1985; 154:1-28.

[21] Shanahan MER. The influence of solid micro-deformation on contact-angle equilibrium. J. Phys. D: Appl. Phys. 1987; 20:945-950.

[22] Butt HJ, Semprebon C, Papadopoulos P, Vollmer D, Brinkmann M, Ciccotti M. Design principles for superamphiphobic surfaces. Soft Matter 2013; 9:418-428.

[23] Drelich JW, Boinovich L, Chibowksi E, Della Volpe C, Holysz L, Marmur A *et al.* Contact angles: history of over 200 years of open questions. Surface Innovations 2020; 8:3-27.** Give a historic overview over the development of research on wetting phenomena.

[24] Pockels A. Über Randwinkel und Ausbreitung von Flüssigkeiten auf festen Körpern. Physikalische Zeitschrift 1914; 15:39-46.

[25] Harkins WD, Brown FE. The determination of surface tension (free surface energy), and the weight of falling drops: The surface tension of water and benzene by the capillary height method. J. Am. Chem. Soc. 1919; 41:499-524.

[26] Sulman HL. Hysteresis of contact-angles. Transactions of the Institution of Mining and Metallurgy 1920; 29:88-97.

[27] Ablett R. An investigation of the angle of contact between paraffin wax and water. Phil. Mag. 1923; 46:244-256.

[28] Adam NK, Jessop G. Angles of contact and polarity of solid surfaces. J. Chem. Soc. 1925; 127:1863-1868.

[29] Eral HB, t'Mannetje DJCM, Oh JM. Contact angle hysteresis: a review of fundamentals and applications. Colloid Polymer Sci. 2013; 291:247-260.

[30] Lhermerout R, Davitt K. Contact angle dynamics on pseudo-brushes: Effects of polymer chain length and wetting liquid. Colloids Surfaces A 2019; 566:148-155.

[31] Gao N, Geyer F, Pilat DW, Wooh S, Vollmer D, Butt H-J *et al.* How drops start sliding over solid surfaces. Nature Physics 2017; 14:191.* Measure the force required to slide a drop over a surface. They note that, like in solid friction, the force required to initiate sliding is higher than the force necessary to maintain sliding.

[32] Zhuravlev LT. The surface chemistry of amorphous silica. Zhuravlev model. Colloids & Surfaces A 2000; 173:1-38.

[33] Shuttleworth R, Bailey GLJ. The spreading of a liquid over a rough solid. Discuss. Faraday Society 1948; 3:16-22.

[34] Johnson RE, Dettre RH, Brandreth DA. Dynamic contact angles and contact angle hysteresis. J. Colloid Interface Sci. 1977; 62:205-212.

[35] Schwartz LW, Garoff S. Contact angle hysteresis on heterogeneous surfaces. Langmuir 1985; 1:219-230.

[36] Marmur A. Soft contact: measurement and interpretation of contact angles. Soft Matter 2006; 2:12-17.

[37] Wu YC, Wang F, Ma SP, Selzer M, Nestler B. How do chemical patterns affect equilibrium droplet shapes? Soft Matter 2020; 16:6115-6127.

[38] Langmuir I. The mechanism of the surface phenomena of flotation. Transactions of the Faraday Society 1920; 15:62-74.

[39] Smith T, Lindberg G. Effect of acoustic energy on contact angle measurements. J. Colloid Interface Sci. 1978; 66:363-366.

[40] Andrieu C, Sykes C, Brochard F. Average spreading parameter on heterogeneous surfaces. Langmuir 1994; 10:2077-2080.

[41] Ruiz-Cabello FJM, Rodriguez-Valverde MA, Cabrerizo-Vilchez MA. Equilibrium contact angle or the most-stable contact angle? Adv. Colloid Interface Sci. 2014; 206:320-327.** They note that vibration of the substrate lead to the formation of a most stable contact angle, which is not necessarily the equilibrium contact angle.

[42] Furmidge CGL. Studies at phase interfaces. I. The sliding of liquid drops on solid surfaces and a theory for spray retention. J. Colloid Sci. 1962; 17:309-324.

[43] Olsen DA, Joyner PA, Olson MD. Sliding of liquid drops on solid surfaces. J. Phys. Chem. 1962; 66:883-886.

[44] Wolfram E, Faust R. Liquid drops on a tilted plate, contact angle hysteresis and the Young contact angle. In: Wetting, Spreading and Adhesion. Padday JF (Editor) New York: Academic Press; 1978. pp. 213-222.

[45] Brown RA, Orr FM, Scriven LE. Static drop on an inclined plane: Analysis by the finite element method. J. Colloid Interface Sci. 1980; 73:76-87.

[46] Extrand CW, Kumagai Y. Liquid drops on an inclined plane: The relation between contact angles, drops hape, and retention forces. J. Colloid Interface Sci. 1995; 170:515-521.* Systematically analyse the influence of drops shape on the lateral capillary force and derive the geometry factor k for different geometries.

[47] Dimitrakopoulos P, Higdon JJL. On the gravitational displacement of three-dimensional fluid droplets from inclined solid surfaces. J. Fluid Mech. 1999; 395:181-209.

[48] ElSherbini A, Jacobi A. Retention forces and contact angles for critical liquid drops on non-horizontal surfaces. J. Colloid Interface Sci. 2006; 299:841-849.

[49] Semprebon C, Brinkmann M. On the onset of motion of sliding drops Soft Matter 2014; 10:3325–3334.

[50] Bartell FE, Wooley AD. Solid-liquid-air contact angles and their dependence upon the surface condition of the solid. J. Amer. Chem. Soc. 1933; 55:3518-3527.

[51] Schäffer E, Wong PZ. Contact line dynamics near the pinning threshold: A capillary rise and fall experiment. Phys. Rev. E 2000; 61:5257-5277.

[52] Johnson RE, Dettre RH. Wettability and contact angles. In: Surface and Colloid Science. Matijevic E (Editor) New York: Wiley - Interscience; 1969. pp. 85-153.

[53] Wang JH, Claesson PM, Parker JL, Yasuda H. Dynamic contact angles and contact angle hysteresis of plasma polymers. Langmuir 1994; 10:3887-3897.

[54] Vergelati C, Perwuelz A, Vovelle L, Romero MA, Holl Y. Poly(ethylene terephthalate) surface dynamics in air and water studied by tensiometry and molecular modelling. Polymer 1994; 35:262-270.

[55] Tretinnikov ON, Ikada Y. Dynamic wetting and contact angle hysteresis of polymer surfaces studied with the modified Wilhelmy balance method. Langmuir 1994; 10:1606-1614.

[56] Rolley E, Guthmann C. Dynamics and hysteresis of the contact line between liquid hydrogen and cesium substrates. Phys. Rev. Lett. 2007; 98:166105.

[57] Perrin H, Lhermerout R, Davitt K, Rolley E, Andreotti B. Thermally activated motion of a contact line over defects. Soft Matter 2018; 14:1581-1595.* Analyse theoretically the influence of a distribution of defects on dynamic advancing and receding contact angles using a Langevin model.

[58] Kim J-H, Kavehpour HP, Rothstein JP. Dynamic contact angle measurements on superhydrophobic surfaces. Phys. Fluids 2015; 27:032107.

[59] Blake TD, Shikhmurzaev YD. Dynamic wetting by liquids of different viscosity. J. Colloid Interface Sci. 2002; 253:196-202.* Present experimental results of dynamic contact angles the measured with the plunging tape setup in water-glycerol mixture. The results of liquids with very different viscosity could be fitted with a theoretical model.

[60] Petrov JG, Ralston J, Schneemilch M, Hayes RA. Dynamics of partial wetting and dewetting in well-defined systems. J. Phys. Chem. B 2003; 107:1634-1645.* Combine the hydrodynamic and molecular-kinetic theories. To verify the combined theory they fit experimental results obtained with various liquids and find good agreement.

[61] Vega MJ, Gouttiere C, Seveno D, Blake TD, Voue M, de Coninck J. Experimental investigation of the link between static and dynamic wetting by forced wetting of nylon filament. Langmuir 2007; 23:10628-10634.

[62] Gaudin AM, Witt AF, Decker TG. Contact angle hysteresis - Principles and application of measurement methods. Trans. AIME 1963; 226:107-112.

[63] Timmons CO, Zisman WA. Effect of liquid structure on contact angle hysteresis. J. Colloid Interface Sci. 1966; 22:165-171.

[64] Holly FJ, Refojo MF. Wettability of hydrogels. I. Poly(2-hydroxyethyl methacrylate). J. Biomed. Mater. Res. 1975; 9:315-326.

[65] Yasuda H, Sharma AK, Yasuda T. Effect of orientation and mobility of polymer molecules at surfaces on contact angle and its hysteresis. J. Polym. Sci. Polym. Phys. Ed. 1981; 19:1285-1291.

[66] Lam CNC, Wu R, Li D, Hair ML, Neumann AW. Study of the advancing and receding contact angles: liquid sorption as a cause of contact angle hysteresis. Adv. Colloid Interface Sci. 2002; 96:169-191.

[67] Wong WSY, Hauer L, Naga A, Kaltbeitzel A, Baumli P, Berger R *et al.* Adaptive wetting of polydimethylsiloxane. Langmuir 2020; 36:7236-7245.

[68] Li X, Silge S, Saal A, Kircher G, Koynov K, Berger R *et al.* Adaptation of a styrene-acrylic acid copolymer surface to water. Langmuir 2021; 37:1571–1577.

[69] Macdougall G, Ockrent C. Surface energy relations in liquid/solid systems. I. The adhesion of liquids to solids and a new method of determining the surface tension of liquids. Proc. Roy. Soc. London A 1942; 180:151-173.

[70] Kawasaki K. Study of wettability of polymers by sliding of a water drop. J. Colloid Sci. 1960; 15:402-407.

[71] Le Grand N, Daerr A, Limat L. Shape and motion of drops sliding down an inclined plane. J. Fluid Mech. 2005; 541:293-315.* They describe for the first the formation of corners and perls at the rear of sliding drops at high velocity.

[72] Olin P, Lindstrom SB, Pettersson T, Wagberg L. Water drop friction on superhydrophobic surfaces. Langmuir 2013; 29:9079-9089.* Image and analyse the sliding of water drops down tilted superhydrophobic surfaces.

[73] Yilbas BS, Al-Sharafi A, Ali H, Al-Aqeeli N. Dynamics of a water droplet on a hydrophobic inclined surface: influence of droplet size and surface inclination angle on droplet rolling. RSC Advances 2017; 7:48806-48818.

[74] Frenkel YI. On the behavior of liquid drops on a solid surface. 1. The sliding of drops on an inclined surface. J. Exptl. Theoret. Phys. (USSR) 1948; 18:659-669.

[75] Kim HY, Lee HJ, Kang BH. Sliding of liquid drops down an inclined solid surface. J. Colloid Interface Sci. 2002; 247:372-380.** Develop analytical equations for the different energies dissipated in sliding drops. They carry out experiments to find out, how much each dissipation meachism contributes.

[76] Rio E, Daerr A, Andreotti B, Limat L. Boundary conditions in the vicinity of a dynamic contact line: Experimental investigation of viscous drops sliding down an inclined plane. Phys. Rev. Lett. 2005; 94:024503.

[77] Goodwin R, Rice D, Middleman S. A model for the onset of motion of a sessile liquid drop on a rotating disk. J. Colloid Interface Sci. 1988; 125:162-169.

[78] Tadmor R, Bahadur P, Leh A, N'guessan HE, Jaini R, Dang L. Measurement of lateral adhesion forces at the interface between a liquid drop and a substrate. Phys. Rev. Lett. 2009; 103:266101.

[79] Evgenidis SP, Kalic K, Kostoglou M, Karapantsios TD. Kerberos: A three camera headed centrifugal/tilting device for studying wetting/dewetting under the influence of controlled body forces. Colloids Surf. A 2017; 521:38-48.

[80] Pilat DW, Papadopoulos P, Schäffel D, Vollmer D, Berger R, Butt H-J. Dynamic measurement of the force required to move a liquid drop on a solid surface. Langmuir 2012; 28:16812-16820.

[81] 't Mannetje D, Banpurkar A, Koppelman H, Duits MHG, van den Ende D, Mugele F. Electrically tunable wetting defects characterized by a simple capillary force sensor. Langmuir 2013; 29:9944-9949.

[82] Daniel D, Timonen JVI, Li RP, Velling SJ, Kreder MJ, Tetreault A *et al.* Origins of extreme liquid repellency on structured, flat, and lubricated hydrophobic surfaces. Phys. Rev. Lett. 2018; 120:244503.

[83] Saal A, Seiler PM, Rettenmaier D, Ade M, Roisman IV, Berger R *et al.* Shuffling gait motion of an aerodynamically driven wall-bound drop. Phys. Rev. Fluids 2020; 5:094006.* In wind tunnel experiments observe that drops in a shuffling gait motion in which temporarily the advancing contact angle can be exceeded.

[84] Dussan EB. On the ability of drops or bubbles to stick to non-horizontal surfaces of solids. 3. The influences of the motion of the surrounding fluid on dislodging drops. J. Fluid Mech. 1987; 174:381-397.

[85] Durbin PA. On the wind force needed to dislodge a drop adhered to a surface. J. Fluid Mech. 1988; 196:205-222.

[86] Milne AJB, Amirfazli A. Drop shedding by shear flow for hydrophilic to superhydrophobic surfaces. Langmuir 2009; 25:14155-14164.

[87] Fan J, Wilson MCT, Kapur N. Displacement of liquid droplets on a surface by a shearing air flow. J. Colloid Interface Sci. 2011; 356:286-292.

[88] Seiler PM, Gloerfeld M, Roisman IV, Tropea C. Aerodynamically driven motion of a wall-bounded drop on a smooth solid substrate. Phys. Rev. Fluids 2019; 4:024001

[89] Blake TD. The physics of moving wetting lines. J. Colloid Interface Sci. 2006; 299:1-13.

[90] Bormashenko EY. Wetting of Real Surfaces. De Gruyter; 2013.

[91] Cassie ABD, Baxter S. Large contact angles of plant and animal surfaces. Nature 1945; 155:21-22.

[92] Neumann AW, Good RJ. Thermodynamics of contact angles. 1. Heterogeneous surfaces. J. Colloid Interface Sci. 1972; 38:341-358.

[93] Swain PS, Lipowsky R. Contact angles on heterogeneous surfaces: A new look at Cassies's and Wezel's laws. Langmuir 1998; 14:6772-6780.

[94] Kusumaatmaja H, Yeomans JM. Modeling contact angle hysteresis on chemically patterned and superhydrophobic surfaces. Langmuir 2007; 23:6019-6032.

[95] Varagnolo S, Schiocchet V, Ferraro D, Pierno M, Mistura G, Sbragaglia M *et al.* Tuning drop motion by chemical patterning of surfaces. Langmuir 2014; 30:2401-2409.

[96] Robbins MO, Joanny JF. Contact angle hysteresis on random surfaces. Europhys. Lett. 1987; 3:729-735.

[97] Nadkarni GD, Garoff S. Reproducibility of contact line motion on surfaces exhibiting contact angle hysteresis. Langmuir 1994; 10:1618-1623. * Are the first ones to observe the dynamics of a moving contact line by reflectance microscopy. They observe all the metastable states of contact lines.

[98] Lhermerout R, Perrin H, Rolley E, Andreotti B, Davitt K. A moving contact line as a rheometer for nanometric interfacial layers. Nature commun. 2016; 7:12545.

[99] Becher-Nienhaus B, Liu GJ, Archer RJ, Hozumi A. Surprising lack of influence on water droplet motion by hydrophilic microdomains on checkerboard-like surfaces with matched contact angle hysteresis. Langmuir 2020; 36:7835-7843.

[100] Adam NK. The Physics and Chemistry of Surfaces. London: Oxford University Press; 1941.

[101] Wenzel RN. Resistance of solid surfaces to wetting by water. Ind. Eng. Chem. 1936; 28:988-994.

[102] Oliver JF, Huh C, Mason SG. An experimental study of some effects of solid surface roughness on wetting. Colloids & Surfaces 1980; 1:79-104.

[103] Quéré D. Wetting and roughness. Annu. Rev. Mater. Res. 2008; 38:71-99.

[104] Bartell FE, Shepard JW. Surface roughness as related to hysteresis of contact angles. I. The system paraffin-water-air. J. Phys. Chem. 1953; 57:211-215.

[105] Dettre RH, Johnson RE. Contact angle hysteresis - porous surfaces. SCI Monograph 1967; 25:144-163.

[106] Cox RG. The spreading of a liquid on a rough solid surface. J. Fluid Mech. 1983; 131:1-26.

[107] Joanny JF, de Gennes PG. A model for contact angle hysteresis. J. Chem. Phys. 1984; 81:552-562.* Develop their theoretical model in which they calculate the shape of a moving contact line around a defect. It is the basis for many more studies to come.

[108] Giacomello A, Schimmele L, Dietrich S. Wetting hysteresis induced by nanodefects. Proc. Natl. Acad. Sci. USA 2016; 113:E262-E271.

[109] Moulinet S, Guthmann C, Rolley E. Roughness and dynamics of a contact line of a viscous fluid on a disordered substrate. Eur. Phys. J. E 2002; 8:437-443.

[110] Reyssat M, Quéré D. Contact angle hysteresis generated by strong dilute defects. J. Phys. Chem. B 2009; 113:3906-3909.* Use hydrophobic micropillar arrays to measure the effect of defects on the apparent receding contact angle.

[111] Butt H-J, Gao N, Papadopoulos P, Steffen W, Kappl M, Berger R. Energy dissipation of moving drops on superhydrophobic and superoleophobic surfaces. Langmuir 2017; 33:107-116.

[112] Thiele U, Knobloch E. Driven drops on heterogeneous substrates: Onset of sliding motion. Phys. Rev. Lett. 2006; 97:204501.

[113] Park J, Kumar S. Droplet sliding on an inclined substrate with a topographical defect. Langmuir 2017; 33:7352-7363.

[114] Nadkarni GD, Garoff S. An investigation of microscopic aspects of contact angle hysteresis - pinning of the contact line on a single defect. Europhys. Lett. 1992; 20:523-528.

[115] Marsh JA, Cazabat AM. Dynamics of contact line depinning from a single defect. Phys. Rev. Lett. 1993; 71:2433-2436.

[116] Joanny JF, de Gennes PG. Physique des surfaces et des interfaces. C. R. Acad. Sc. Paris 1984; 299:279-283.

[117] Carré A, Gastel JC, Shanahan MER. Viscoelastic effects in the spreading of liquids. Nature 1996; 379:432-434.

[118] Pericet-Camara R, Best A, Butt H-J, Bonaccurso E. Effect of capillary pressure and surface tension on the deformation of elastic surfaces by sessile liquid microdrops: An experimental investigation. Langmuir 2008; 24:10565-10568.

[119] Park SJ, Weon BM, Lee JS, Lee J, Kim J, Je JH. Visualization of asymmetric wetting ridges on soft solids with X-ray microscopy. Nature commun. 2014; 5:4369-4369.

[120] van Gorcum M, Andreotti B, Snoeijer JH, Karpitschka S. Dynamic solid surface tension causes droplet pinning and depinning. Phys. Rev. Lett. 2018; 121:208003.*Analyse the stick-slip movement of contact lines on soft PDMS surfaces. They explain their observation by an increase of the solid surface energy rather than rheology.

[121] Shanahan MER, de Gennes PG. The ridge produced by a liquid near the triple line solid/liquid/fluid. C. R. Acad. Sc. Paris Serie II 1986; 302:517-521.

[122] Rusanov AI. Theory of the wetting of elastically deformed bodies. 1. Deformation with a finite contact angle. Colloid J. USSR 1975; 37:614-622.

[123] Style RW, Dufresne ER. Static wetting on deformable substrates, from liquids to soft solids. Soft Matter 2012; 8:7177-7184. * Analyse drops on very soft substrates and introdcue their comparison with drops on liquid surfaces. The paper led to many following studies on elastocapillary wetting.

[124] Style RW, Che Y, Park SJ, Weon BM, Je JH, Hyland C *et al.* Patterning droplets with durotaxis. Proc. Natl. Acad. Sci. USA 2013; 110:12541-12544.

[125] Extrand CW, Kumagai Y. Contact angles and hysteresis on soft surfaces. J. Colloid Interface Sci. 1996; 184:191-200.

[126] Limat L. Straight contact lines on a soft, incompressible solid. Eur. Phys. J. E 2012; 35:134.

[127] Carré A, Shanahan MER. Viscoelastic breaking of a running drop. Langmuir 2001; 17:2982-2985.

[128] Pu G, Severtson SJ. Characterization of dynamic stick-and-break wetting behavior for various liquids on the surface of a highly viscoelastic polymer. Langmuir 2008; 24:4685-4692.

[129] Kajiya T, Daerr A, Narita T, Royon L, Lequeux F, Limat L. Advancing liquid contact line on visco-elastic gel substrates: stick-slip vs. continuous motions. Soft Matter 2013; 9:454-461.

[130] Dervaux J, Roche M, Limat L. Nonlinear theory of wetting on deformable substrates. Soft Matter 2020; 16:5157-5176.

[131] Andreotti B, Snoeijer JH. Statics and dynamics of soft wetting. Annual Reviews Fluid Mechanics 2020; 52:285-308.* Summarises the knowledge of dynamic wetting of soft substrates.

[132] van Gorcum M, Karpitschka S, Andreotti B, Snoeijer JH. Spreading on viscoelastic solids: are contact angles selected by Neumann's law? Soft Matter 2020; 16:1306-1322.

[133] Edser E. The concentration of minerals by flotation. In: Fourth Report on Colloid Chemistry and its General and Industrial Applications. Science BAftAo (Editor) London: His Majesty's Stationary Office; 1922. pp. 263-326.

[134] Lavielle L, Schultz J. Surface properties of graft polyethylene in contact with water. I. Orientation phenomena. J. Colloid Interface Sci. 1985; 106:438-445.

[135] Yasuda T, Miyama M, Yasuda H. Dynamics of the surface configuration change of polymers in response to changes in environmental conditions. 2. Comparison of changes in air and in liquid water. Langmuir 1992; 8:1425-1430.

[136] Vaidya A, Chaudhury MK. Synthesis and surface properties of environmentally responsive segmented polyurethanes. J. Colloid Interface Sci. 2002; 249:235–245.

[137] Crowe JA, Genzer J. Creating responsive surfaces with tailored wettability switching kinetics and reconstruction reversibility. J. Am. Chem. Soc. 2005; 127:17610-17611.

[138] Hanni-Ciunel K, Findenegg GH, von Klitzing R. Water contact angle on polyelectrolyte-coated surfaces: Effects of film swelling and droplet evaporation. Soft Materials 2007; 5:61-73.

[139] Grundke K, Poschel K, Synytska A, Frenzel R, Drechsler A, Nitschke M *et al.* Experimental studies of contact angle hysteresis phenomena on polymer surfaces - Toward the understanding and control of wettability for different applications. Adv. Colloid Interface Sci. 2015; 222:350-76.

[140] Tokarev I, Minko S. Stimuli-responsive hydrogel thin films. Soft Matter 2009; 5:511-524.

[141] Chen L, Liu MJ, Lin L, Zhang T, Ma J, Song YL *et al.* Thermal-responsive hydrogel surface: tunable wettability and adhesion to oil at the water/solid interface. Soft Matter 2010; 6:2708-2712.

[142] Minko S, Müller M, Motornov M, Nitschke M, Grundke K, Stamm M. Two-level structured self-adaptive surfaces with reversibly tunable properties. J. Am. Chem. Soc. 2003; 125:3896-3900.

[143] Zhao B, He T. Synthesis of well-defined mixed poly(methyl methacrylate) / polystyrene brushes from an asymmetric difunctional initiator-terminated self-assembled monolayer. Macromolecules 2003; 36:8599-8602.

[144] Brown AA, Azzaroni O, Fidalgo LM, Huck WTS. Polymer brush resist for responsive wettability. Soft Matter 2009; 5:2738-2745.

[145] Sui X, Zapotoczny S, Benetti EM, Memesa M, Hempeniusa MA, Vancso GJ. Grafting mixed responsive brushes of poly(N-isopropylacrylamide) and poly(methacrylic acid) from gold by selective initiation. Polym. Chem. 2011; 2:879-884.

[146] Tonhauser C, Golriz AA, Moers C, Klein R, Butt H-J, Frey H. Stimuli-responsive Y-shaped polymer brushes based on junction-point-reactive block copolymers. Adv. Mater. 2012; 24:5559-5563.

[147] Ionov L, Minko S. Mixed polymer brushes with locking switching. ACS Appl. Materials & Interfaces 2012; 4:483-489.

[148] Ochsmann JW, Lenz S, Lellig P, Emmerling SGJ, Golriz AA, Reichert P *et al.* Stress-structure correlation in PS-PMMA mixed polymer brushes. Macromolecules 2012; 45:3129-3136.

[149] Hansen RS, Miotto M. Relaxation phenomena and contact angle hysteresis. J. Am. Chem. Soc. 1957; 79:1765-1765.

[150] Elliott GEP, Riddiford AC. Dynamic contact angles.1. Effect of impressed motion. J. Colloid Interface Sci. 1967; 23:389-398.

[151] Starov VM, Velarde MG, Radke CJ. Wetting and Spreading Dynamics. London: CRC Press; 2007. 515 p.

[152] Lee KS, Ivanova N, Starov VM, Hilal N, Dutschk V. Kinetics of wetting and spreading by aqueous surfactant solutions. Adv. Colloid Interface Sci. 2008; 144:54-65.

[153] Luokkala BB, Garoff S, Tilton RD, Suter RM. Interfacial structure and rearrangement of nonionic surfactants near a moving contact line. Langmuir 2001; 17:5917-5923.

[154] Fell D, Auernhammer G, Bonaccurso E, Liu CJ, Sokuler R, Butt HJ. Influence of surfactant concentration and background salt on forced dynamic wetting and dewetting. Langmuir 2011; 27:2112-2117.

[155] Henrich F, Fell D, Truszkowska D, Weirich M, Anyfantakis M, Nguyen TH *et al.* Influence of surfactants in forced dynamic dewetting. Soft Matter 2016; 12:7782-7791.

[156] Butt H-J, Berger R, Steffen W, Vollmer D, Weber SAL. Adaptive wetting - adaptation in wetting. Langmuir 2018; 34:11292−11304.* Summarizes the influence of adapation on wetting and presents a phenomenological model, which links the adapation kinetics to changes in dynamic contact angles.

[157] Bonn D, Eggers J, Indekeu J, Meunier J, Rolley E. Wetting and spreading. Rev. Modern Physics 2009; 81:739-805.

[158] Joanny JF, Robbins MO. Motion of a contact line on a heterogeneous surface. J. Chem. Phys. 1990; 92:3206-3212.

[159] Xu XM, Wang XP. Theoretical analysis for dynamic contact angle hysteresis on chemically patterned surfaces. Phys. Fluids 2020; 32:112102.

[160] Blake TD, Haynes JM. Kinetics of liquid/liquid displacement. J. Colloid Interface Sci. 1969; 30:421-423.

[161] Cherry BW, Holmes CM. Kinetics of wetting of surfaces by polymers. J. Colloid Interface Sci. 1969; 29:174-176.

[162] Snoeijer JH, Andreotti B. Moving contact lines: Scales, regimes, and dynamical transitions. Ann. Rev. Fluid Mech. 2013; 45:269-292.

[163] Perrin H, Lhermerout R, Davitt K, Rolley E, Andreotti B. Defects at the nanoscale impact contact line motion at all scales. Phys. Rev. Lett. 2016; 116:184502.

[164] Ramiasa M, Ralston J, Fetzer R, Sedev R, Fopp-Spori DM, Morhard C *et al.* Contact line motion on nanorough surfaces: A thermally activated process. J. Am. Chem. Soc. 2013; 135:7159-7171.

[165] Davitt K, Pettersen MS, Rolley E. Thermally activated wetting dynamics in the presence of surface roughness. Langmuir 2013; 29:6884-6894.

[166] Huh C, Scriven LE. Hydrodynamic model of steady movement of a solid/liquid/fluid contact line. J. Colloid Interface Sci. 1971; 35:85-101.

[167] Voinov OV. Hydrodynamics of wetting. Fluid Dynamics 1976; 11:714-721.

[168] Cox RG. The dynamics of the spreading of liquids on a solid surface. Part 1. Viscous flow. J. Fluid Mech. 1986; 168:169-194.

[169] Dussan EB, Ramé E, Garoff S. On identifying the appropriate boundary conditions at a moving contact line: an experimental investigation. J. Fluid Mech. 1991; 230:97-116.

[170] Eggers J. Existence of receding and advancing contact lines. Phys. Fluids 2005; 17:082106.

[171] Snoeijer JH. Free-surface flows with large slopes: Beyond lubrication theory. Physics of Fluids 2006; 18:021701.

[172] Maglio M, Legendre D. Numerical simulation of sliding drops on an inclined solid surface. In: Computational and Experimental Fluid Mechanics with Applications to Physics, Engineering and the Environment. Sigalotti LD, Klapp J, Sira E (Editors). 2014. pp. 47-69.

[173] Marsh JA, Garoff S, Dussan EB. Dynamic contact angles and hydrodynamics near a moving contact line. Phys. Rev. Lett. 1993; 70:2778-2781.

[174] Huh C, Mason SG. The steady movement of a liquid meniscus in a capillary tube. J. Fluid Mech. 1977; 81:401-419.

[175] Hocking LM. A moving fluid interface. Part 2. The removal of the force singularity by a slip flow. J. Fluid Mech. 1977; 79:209-229.

[176] Dussan EB. On the spreading of liquids on solid surfaces: Static and dynamic contact lines. Ann. Rev. Fluid Mech. 1979; 11:371-400.

[177] Ruckenstein E, Dunn CS. Slip velocity during wetting of solids. J. Colloid Interface Sci. 1977; 59:135.

[178] Koplik J, Banavar JR, Willemsen JF. Molecular dynamics of fluid flow at solid surfaces. Phys. Fluids A 1989; 1:781-794.

[179] Thompson PA, Robbins MO. Simulations of contact-line motion: Slip and the dynamic contact angle. Phys. Rev. Lett. 1989; 63:766-769.

[180] Blake TD, Fernandez-Toledano JC, Doyen G, De Coninck J. Forced wetting and hydrodynamic assist. Phys. Fluids 2015; 27:112101

[181] Cox RG. The dynamics of the spreading of liquids on a solid surface. Part 2. Surfactants. J. Fluid Mech. 1986; 168:195-220.

[182] Fernández-Toledano JC, Blake TD, De Coninck J. Taking a closer look: A molecular-dynamics investigation of microscopic and apparent dynamic contact angles. J. Colloid Interface Sci. 2021; 587:311-323.** Use molecular dynamics simulations to obtain advancing and receding contact angles versus velocity for the first time.

[183] Petrov PG, Petrov JG. A combined molecular-hydrodynamic appraoch to wetting kinetics. Langmuir 1992; 8:1762-1767.

[184] Brochard-Wyart F, de Gennes PG. Dynamics of partial wetting. Adv. Colloid Interface Sci. 1992; 39:1-11.

[185] Prevost A, Rolley E, Guthmann C. Thermally activated motion of the contact line of a liquid ^{4}He meniscus on a cesium substrate. Phys. Rev. Lett. 1999; 83:348-351.

[186] Petrov JG, Petrov PG. Forced advancement and retraction of polar liquids on a low energy surface. Colloids & Surfaces 1992; 64:143-149.

[187] Chen W, Fadeev AY, Hsieh MC, Öner D, Youngblood J, McCarthy TJ. Ultrahydrophobic and ultralyophobic surfaces: Some comments and examples. Langmuir 1999; 15:3395-3399.

[188] Wang LM, McCarthy TJ. Covalently attached liquids: Instant omniphobic surfaces with unprecedented repellency. Angew. Chem. Int. Ed. 2016; 55:244-248.** By grafting PDMS from surfaces they achieve very low contact angle hysteresis.

[189] Huang SL, Li J, Liu L, Zhou LD, Tian XL. Lossless fast drop self-transport on anisotropic omniphobic surfaces: Origin and elimination of microscopic liquid residue. Advanced Materials 2019; 31:1901417.

[190] Wooh S, Vollmer D. Silicone brushes: Omniphobic surfaces with low sliding angles. Angew. Chem. Int. Ed. 2016; 55:6822-6824.* Review methods to fabricate surfaces with low contact angle hystereis by attaching flexible polymers such as PDMS to the surface.

[191] Cha H, Vahabi H, Wu A, Chavan S, Kim MK, Sett S *et al.* Dropwise condensation on solid hydrophilic surfaces. Science Advances 2020; 6:eaax0746.

[192] Cheng DF, Urata C, Yagihashi M, Hozumi A. A statically oleophilic but dynamically oleophobic smooth nonperfluorinated surface. Angew. Chem. Int. Ed. 2012; 51:2956-2959.

[193] Liu J, Sun YL, Zhou XT, Li XM, Kappl M, Steffen W *et al.* One-step synthesis of a durable and liquid-repellent poly(dimethylsiloxane) coating. Advanced Materials 2021; 33: 2100237.* Present a new, simple method to graft PDMS from surfaces and achieve low contact hysteresis.

[194] Wooh S, Encinas N, Vollmer D, Butt HJ. Stable hydrophobic metal-oxide photocatalysts via grafting polydimethylsiloxane brush. Adv. Mater. 2017; 29:1604637.

[195] Teisala H, Baumli P, Weber SAL, Vollmer D, Butt HJ. Grafting silicone at room temperature - a transparent, scratch-resistant nonstick molecular coating. Langmuir 2020; 36:4416-4431.

[196] Inutsuka M, Tanoue H, Yamada NL, Ito K, Yokoyama H. Dynamic contact angle on a reconstructive polymer surface by segregation. RSC Advances 2017; 7:17202-17207.

[197] Wong TS, Kang SH, Tang SKY, Smythe EJ, Hatton BD, Grinthal A *et al.* Bioinspired self-repairing slippery surfaces with pressure-stable omniphobicity. Nature 2011; 477:443-447.

[198] Lafuma A, Quere D. Slippery pre-suffused surfaces. EPL 2011; 96:56001.

[199] Schellenberger F, Xie J, Encinas N, Hardy A, Klapper M, Papadopoulos P *et al.* Direct observation of drops on slippery lubricant-infused surfaces. Soft Matter 2015; 11:7617-7626.* First confocal microscope images of drops on lubricant-infused surfaces. Such 3D images allow a better interpretaion of contact angles on such surfaces.

[200] Semprebon C, McHale G, Kusumaatmaja H. Apparent contact angle and contact angle hysteresis on liquid infused surfaces. Soft Matter 2017; 13:101-110.* Clarify the role of apparent and local contact angles for drops on liquid-infused surfaces.

[201] Quéré D. Non-sticking drops. Rep. Prog. Phys. 2005; 68:2495-2532.

[202] Smith JD, Dhiman R, Anand S, Reza-Garduno E, Cohen RE, McKinley GH *et al.* Droplet mobility on lubricant-impregnated surfaces. Soft Matter 2013; 9:1772-1780.

[203] Liu H, Zhang P, Liu M, Wang S, Jiang L. Organogel-based thin films for self-cleaning on various surfaces. Adv. Mater. 2013; 25:4477-4481.

[204] Eifert A, Paulssen D, Varanakkottu SN, Baier T, Hardt S. Simple fabrication of robust water-repellent surfaces with low contact-angle hysteresis based on impregnation. Adv. Mater. Interf. 2014; 1:1300138.* Describe a simple method to coat surfaces with PDMS and demonstrate that contact angle hysteresis can be further reduced by adding a lubricant.

[205] Peppou-Chapman S, Hong JK, Waterhouse A, Neto C. Life and death of liquid-infused surfaces: a review on the choice, analysis and fate of the infused liquid layer. Chemical Society Reviews 2020; 49:3688-3715.

[206] Keiser A, Keiser L, Clanet C, Quéré D. Drop friction on liquid-infused materials. Soft Matter 2017; 13:6981-6987.

[207] Keiser A, Baumli P, Vollmer D, Quéré D. Universality of friction laws on liquid-infused materials. Phys. Rev. Fluids 2020; 5:014005.

[208] Cai ZY, Skabeev A, Morozova S, Pham JT. Fluid separation and network deformation in wetting of soft and swollen surfaces. Communications Materials 2021; 2:21.

[209] Gerber J, Lendenmann T, Eghlidi H, Schutzius TM, Poulikakos D. Wetting transitions in droplet drying on soft materials. Nature Communications 2019; 10:4776.

[210] Daniel D, Timonen JVI, Li RP, Velling SJ, Aizenberg J. Oleoplaning droplets on lubricated surfaces. Nature Physics 2017; 13:1020-1025.* Analyse forces required to slide a drop on a liquid-infused surface. They combine it with reflectance interference microscopy to relate the forces to the state of the liquid film underneath a drop on a lubricant-infused surfaces.

[211] Extrand CW. Criteria for ultralyophobic surfaces. Langmuir 2004; 20:5013-5018.

[212] Zheng QS, Yu Y, Zhao ZH. Effects of hydraulic pressure on the stability and transition of wetting modes of superhydrophobic surfaces. Langmuir 2005; 21:12207-12212.

[213] Sakai M, Song JH, Yoshida N, Suzuki S, Kameshima Y, Nakajima A. Direct observation of internal fluidity in a water droplet during sliding on hydrophobic surfaces. Langmuir 2006; 22:4906-4909.* Use a high-speed camera and particle image velocimetry to image the flow inside sliding drops. The can distinuish rolling and sliding components in the flow.

[214] Rathgen H, Mugele F. Microscopic shape and contact angle measurement at a superhydrophobic surface. Faraday Discussions 2010; 146:49-56.

[215] Herminghaus S. Roughness-induced non-wetting. Europhys. Lett. 2000; 52:165-170.

[216] Tuteja A, Choi W, Ma ML, Mabry JM, Mazzella SA, Rutledge GC *et al.* Designing superoleophobic surfaces. Science 2007; 318:1618-1622.

[217] Schellenberger F, Encinas N, Vollmer D, Butt H-J. How water advances on superhydrophobic surfaces. Phys. Rev. Lett. 2016; 116:6101.*Demonstrate by confocal microscopy that on superhydrophobic surface water advances by a touch down at the front and an instability of liquid bridges at the rear. The real advancing contact angle is 180°.

Declaration of interests

☒ The authors declare that they have no known competing financial interests or personal relationships that could have appeared to influence the work reported in this paper.

☐The authors declare the following financial interests/personal relationships which may be considered as potential competing interests: